Mechanical characterization and cleaning of CVD single-layer h-BN resonators

Santiago J. Cartamil-Bueno[1], Matteo Cavalieri[1], Ruizhi Wang[2], Samer Houri[1], Stephan Hofmann[2] & Herre S. J. van der Zant[1]

[1]*Kavli Institute of Nanoscience, Delft University of Technology, Lorentzweg 1, 2628CJ, Delft, The Netherlands*

[2]*Department of Engineering, University of Cambridge, 9 JJ Thomson Avenue, CB30FA, Cambridge, United Kingdom*

Supplementary Information

Supplementary Information Outline:

1. AFM and SEM images of the CVD single-layer h-BN resonators.

2. Raman spectrum before and after cleaning.

3. Distribution of the mechanical properties of the measured devices at room temperature.

4. Temperature dependence of the resonance frequency and quality factor.

5. Complete dataset of fundamental frequencies and quality factor.

AFM and SEM images of the CVD single-layer h-BN resonators.

The mechanical devices are characterized by means of Atomic Force Microscopy (Figure S-1) and Scanning Electron Microscopy (Figure S-2). AFM is used in Peak Force mode to scan the topography of the suspended structures.

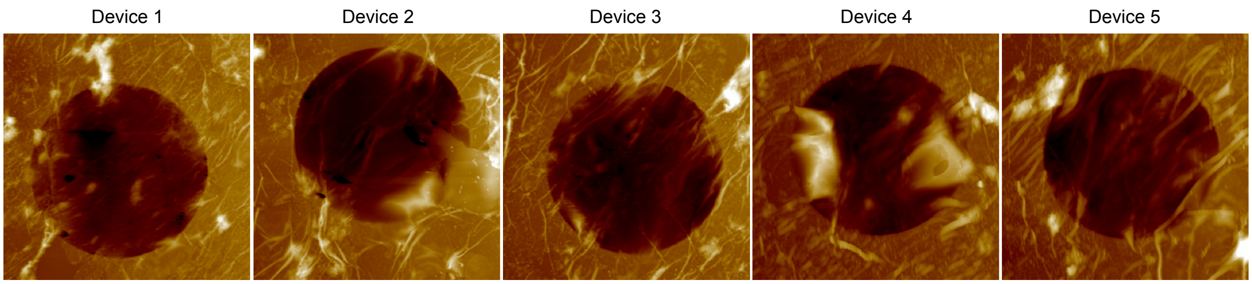

Figure S-1: AFM images of single-layer h-BN mechanical devices before cleaning. Devices are 5 μm in diameter.

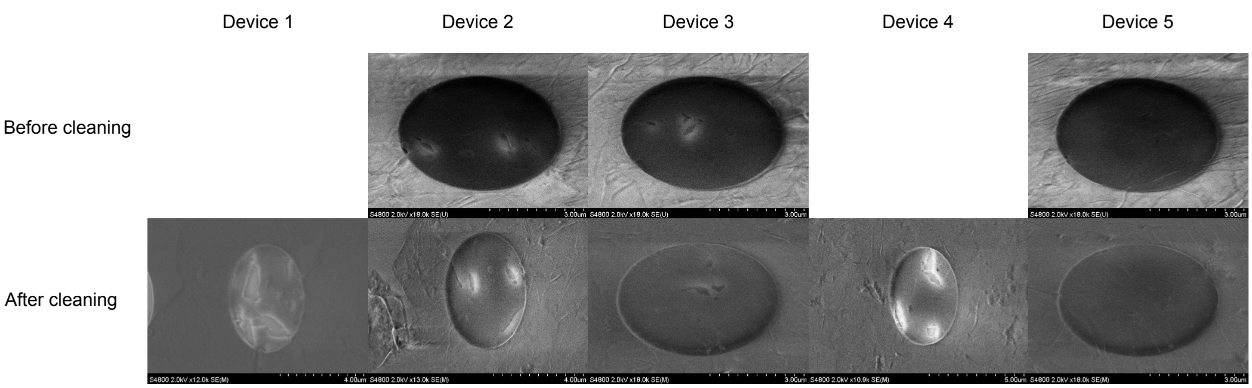

Figure S-2: SEM images of single-layer h-BN mechanical devices before and after cleaning in harsh environments.

Raman spectrum before and after cleaning

Raman spectroscopy on the h-BN material over Si/SiO_2 was carried out with the a Renishaw in Via Raman microscope. Measurements with a laser light of 514 nm were performed on supported areas. The backscattered light was collected with a 100× objective (NA = 0.95) and recorded with a 1800 lines/mm grating, which gives a spectral resolution of ∼1.75 cm^{-1}. The laser power was about 25 mW. Figure S-3a shows the Raman spectrum before the cleaning. The single-layer h-BN peak is visible over the contamination 'bump'. Figure S-3b shows the Raman spectrum of h-BN with a contamination features after the oven annealing in air at 450°C. Figure S-3c shows the Raman spectrum of the material without the contamination signature as result of the cleaning in ozone environment for 30 minutes.

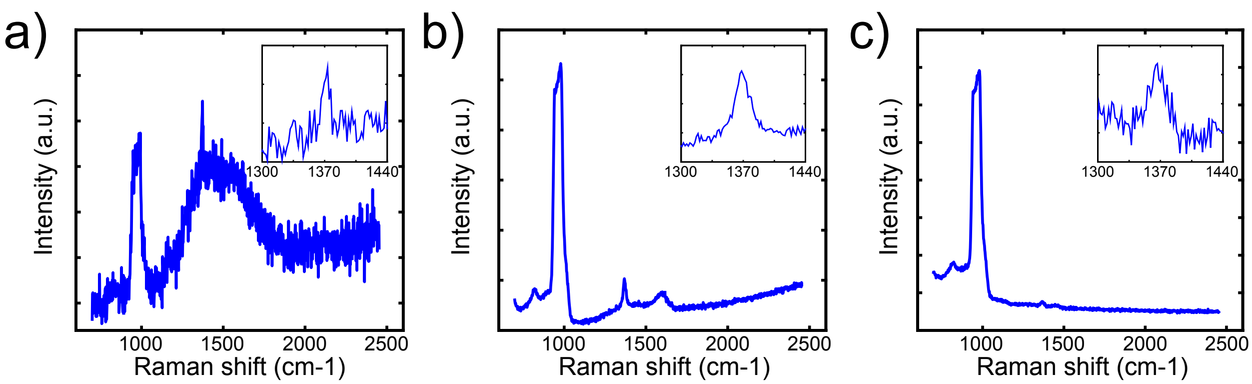

Figure S-3: Raman spectrum of the h-BN material (a) before cleaning, (b) after oven annealing, and (c) after ozone cleaning.

Distribution of the mechanical properties of the measured devices at room temperature.

Figure 4 displays the data presented in Table 1 and 2 in the main text. Figure 4a shows the tension and Young's modulus of the 5 different devices of 5 μm in diameter measured by AFM indentation. Device 5 has a larger Young's modulus than the other devices possibly due to the lack of small perforations in the membrane. Figure 4b shows the tension of the same devices when using the laser interferometer before and after the cleaning processes. There is a clear trend in the devices to increase the tension after each consecutive cleaning process.

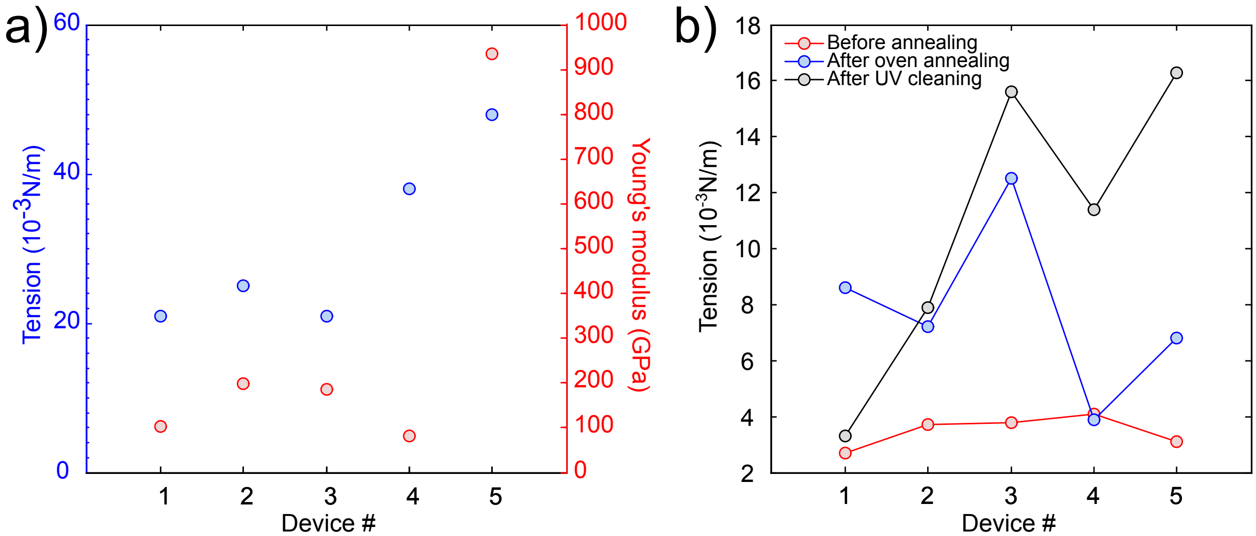

Figure S-4: Mechanical properties of the devices at room temperature. a) Tension and Young's modulus values determined from AFM nanoindentation measurements (Table 1 in main text). b) Tension values from the laser interferometric technique before and after cleaning in harsh environments (Table 2 in main text).

Temperature dependence of the resonance frequency and quality factor.

When cooling a resonator, the resonance frequency and quality factor increases as pictured in Figure S-5. Figure S-6 shows the dependence of the mechanical properties with temperature. The dissipation (Q^{-1}) in these kind of systems has a low-temperature $T^{1/3}$ and high-temperature T^2 or T^3 power-law dependences, which are still not understood [S-1][S-2]. From Figure S-3b we obtain an low-temperature dependence of $T^{0.49}$, $T^{0.22}$, and $T^{0.07}$ for the h-BN drums before cleaning (red circles), after annealing (blue circles), and after ozone cleaning (black circles), respectively. The high-temperature power-law dependence for those cases become $T^{2.10}$, $T^{0.82}$, and $T^{0.76}$.

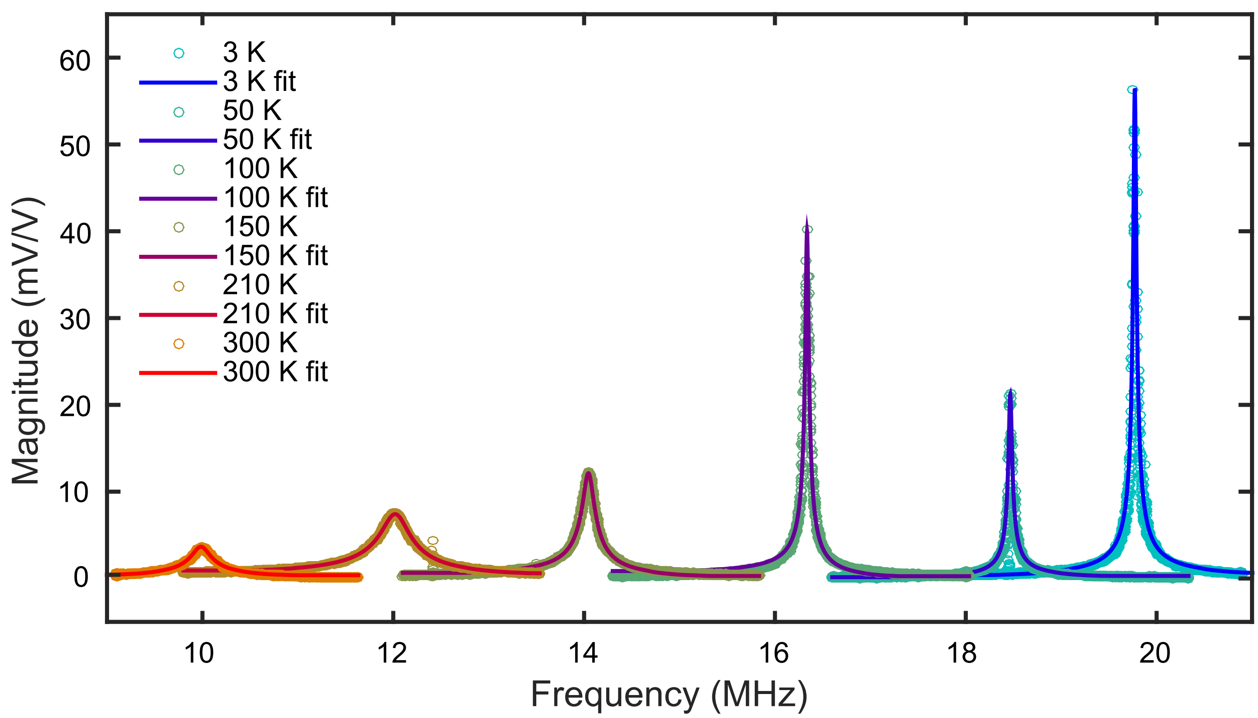

Figure S-5: Evolution of the fundamental resonance frequency with temperature for a h-BN drum before cleaning (device 3).

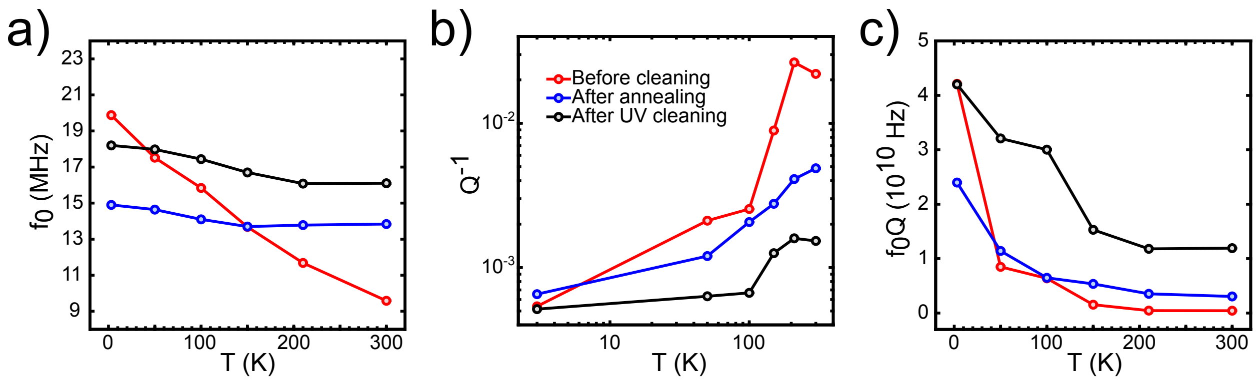

Figure S-6: Temperature dependence of the mechanical properties for the h-BN drums before cleaning, after oven annealing, and after UV ozone cleaning. a) Averaged frequency versus temperature. b) Averaged dissipation versus temperature. c) Averaged f_0Q product versus temperature.

Complete dataset of fundamental frequencies and quality factor.

The tables in .xls files collect all the data from the temperature measurements for the samples before cleaning (table S-1), after oven annealing (table S-2), and after UV-induced ozone cleaning (table S-3).

References

[S-1] Zande AM van der, Barton RA, Alden JS, *et al*. Large-Scale Arrays of Single-Layer Graphene Resonators. *Nano Letters* 2010; 10: 48694873.

[S-2] Chen C, Rosenblatt S, Bolotin KI, *et al*. Performance of monolayer graphene nanomechanical resonators with electrical readout. *Nature Nanotechnology* 2009; 4: 861867.